Research Square

Preprints are preliminary reports that have not undergone peer review.
They should not be considered conclusive, used to inform clinical practice,
or referenced by the media as validated information.

Speciation and bioavailability of Pb, Cr, As and Zn in agricultural soils with and without mining history in the Ecuadorian Amazon

Yandry Bermello
Universidad Regional Amazónica Ikiam
Samantha Jiménez-Oyola
ESPOL Polytechnic University
Oswaldo Guzmán
Universidad Regional Amazónica Ikiam
Cindy Goyburo-Chávez
ESPOL Polytechnic University
Anderson Guamán
Universidad Regional Amazónica Ikiam
Ehiner Tapia
Universidad Regional Amazónica Ikiam
Santiago Balcázar-Loaiza
santiago.balcazar@ikiam.edu.ec

Universidad Regional Amazónica Ikiam

Research Article

Keywords: Soil monitoring, Sequential extraction, Redox conditions, Metal(loid) mobility, Risk assessment

Posted Date: June 19th, 2026

DOI: https://doi.org/10.21203/rs.3.rs-9901810/v1

License: This work is licensed under a Creative Commons Attribution 4.0 International License.
Read Full License

Additional Declarations: No competing interests reported.

Abstract

Agricultural soils in the Ecuadorian Amazon may be affected by both geogenic processes and mining-related disturbances, raising concerns about metal(loid) mobility, bioavailability, and potential transfer to crops. This study assessed selected agricultural soils from the upper Anzu watershed, where farms with and without mining history occur under comparable geological and edaphic conditions. Soil samples were analyzed for physicochemical properties, pseudo-total concentrations of Pb, Cr, As, and Zn by portable X-ray fluorescence, Pb fractionation using the Tessier sequential extraction procedure, and pH–Eh-based geochemical speciation. Metal(loid) concentrations showed limited spatial variability, with Cr and Zn as the most abundant elements, while Pb and As occurred at lower concentrations. No statistically clear separation was observed between farms with and without mining history, suggesting that metal distribution is mainly controlled by shared edaphic and lithological conditions. Pb fractionation indicated a predominance of the exchangeable fraction in selected samples, pointing to high potential mobility and bioavailability under acidic soil conditions. Thermodynamic interpretation suggests that Pb and Zn may occur mainly as mobile divalent cations, whereas Cr is stabilized predominantly as Cr(III). Arsenic behavior appears strongly controlled by redox conditions, with arsenate ($H_2AsO_4^-$) predicted under the measured conditions, although direct speciation analyses would be required for confirmation. Overall, the results highlight the need to integrate total concentrations with speciation and bioavailability indicators for environmental monitoring and risk assessment in tropical agricultural landscapes.

1. Introduction

The Amazon basin is the world's largest tropical rainforest and one of its most biodiverse regions, increasingly threatened by extractive activities that compromise water, sediment, and soil quality (Strand et al., 2018). Within this context, the Ecuadorian Amazon has experienced a recent expansion of alluvial gold mining across several sub-watersheds of the Sub-Andean Zone, often overlapping with traditional agricultural lands (Moulatlet et al., 2023).

On alluvial terraces of the upper Napo basin, smallholder farmers cultivate cassava, plantain, cacao, and citrus on lands that, in some cases, have been alternately used for agriculture and gold extraction (Rivera-Rhon & Bravo-Grijalva, 2023; Vasco-Viteri et al., 2023). Once mining ceases, these lands typically return to crop production without prior assessment of soil contamination, creating uncertainty regarding crop safety and human exposure to potentially toxic elements. Although recent studies have evaluated the occurrence of metal(loid)s in Amazonian waters and active sediments (Capparelli et al., 2020; Galarza et al., 2021; Jiménez et al., 2021; Montoya et al., 2025), agricultural soils have received markedly less attention, despite acting as long-term sinks and potential sources of contaminants in the trophic chain (Angon et al., 2024; Ríos Guayasamín et al., 2024)

Lead (Pb), chromium (Cr), arsenic (As), and zinc (Zn) are among the most environmentally relevant metal(loid)s in mining-influenced soils due to their toxicity, persistence, and bioaccumulation potential

(Barra Caracciolo & Terenzi, 2021; Campillo-Cora et al., 2025). In Amazonian aquatic systems of the upper Napo basin, metal concentrations often approach or exceed background levels typical of the Amazon basin, with geological factors such as black shale weathering and active volcanism identified as primary controls of regional patterns (Montoya et al., 2025; Tapia Cordero, 2024).

However, total concentrations alone are insufficient to evaluate ecological or human-health risk, because the fraction effectively available for plant uptake or microbial interaction depends on chemical speciation rather than bulk content (Ramos et al., 2022; Vila, 2018; Wang et al., 2025). Speciation and bioavailability are governed by intrinsic soil properties, particularly pH, redox potential (Eh), and organic matter content, which control sorption, complexation, and the stability of soluble species (Bourg & Loch, 1995; Karimian et al., 2018; Vila, 2018). Two complementary approaches are commonly used to characterize this behavior: indirect thermodynamic prediction through Pourbaix (Eh–pH) diagrams, and direct operational fractionation through sequential extraction procedures such as the Tessier method (Tessier et al., 1979; Woszczyk et al., 2018; Vilar et al., 2003; von Gunten, 2024).

In the upper Anzu River watershed (Napo Province, Ecuadorian Amazon), alluvial soils developed from the weathering of the Middle Jurassic Abitagua Granite share a common lithogenic background, providing a setting in which the relative contributions of geogenic versus anthropogenic (mining) inputs can be evaluated (Aspden et al., 1992; Vera-Jaramillo et al., 2026). To date, however, no study has compared agricultural soils with and without a history of mining activity under such comparable geological conditions.

This study evaluates the total concentration, geochemical speciation, and bioavailability of Pb, Cr, As, and Zn in agricultural soils from farms with and without mining history in the upper Anzu watershed. The specific objectives were to: (i) quantify the pseudo-total concentrations of the four elements in both farm types; (ii) determine the dominant chemical species and bioavailable fractions through Pourbaix diagrams and the Tessier sequential extraction procedure; and (iii) relate the intrinsic soil properties (pH, Eh, electrical conductivity, and soil organic matter) to metal(loid) mobility.

2. Materials and methods

Study area

The study was conducted in the Carlos Julio Arosemena Tola canton, Napo Province, in the northern Ecuadorian Amazon (Fig. 1a). According to the National Cadastre, 47 mining concessions are currently registered within the study area, frequently overlapping with active agricultural lands (Conali, 2020). The local climate corresponds to the Upper Amazon, with annual precipitation exceeding 3000–3500 mm, mean annual temperatures of 22–26°C, and high humidity throughout the year (INAMHI, 2025).

The study area lies within the northern Ecuadorian Amazon, where the surficial geology is dominated by recent alluvial deposits derived from the weathering and erosion of the surrounding bedrock (Fig. 2). These Quaternary deposits overlie a sequence of Cenozoic sedimentary formations (Mesa, Chambira,

Arajuno, Chalcana, Tiyuyacu, Tena, and Napo), which consist primarily of limestones, sandstones, siltstones, and claystones deposited in marine, fluvial, and transitional environments (Baby et al., 2004; Christophoul et al., 2002; Gutiérrez et al., 2019)

The primary lithogenic source for the Quaternary deposits is the Abitagua Granite, a Middle Jurassic (~ 162 Ma) batholith (Aspden et al., 1992; Vera-Jaramillo et al., 2026). This granitic unit forms part of an extensive Jurassic magmatic belt in the Sub-Andean Zone and is classified as an I-type granitoid (Aspden et al., 1992; Litherland & Viteri, 1994). Its mineral assemblage, dominated by quartz, K-feldspar, plagioclase, biotite, and amphibole, includes accessory phases such as chlorite and epidote (Guzman & Campos, 2024; Huatatoca-mamallacta et al., 2025; Vera et al., 2023), which can be natural hosts for various trace elements, including heavy metals. Consequently, the agricultural soils sampled in this study, developed from recent alluvial materials, have a direct genetic link to the Abitagua Granite through the intermediate sedimentary cycle. This geological framework establishes the granitic basement as the dominant natural (geogenic) source for the soil matrix and its inherent geochemical background.

Four agricultural farms were selected: two without any history of mining activity and two with documented past mining intervention. Three composite soil samples were collected from each farm, resulting in six control samples (C-01 to C-06) and six mining-history samples (M-01 to M-06). All four farms are located on alluvial terraces of comparable elevation, slope, and parent material, with similar crop rotations and management practices, minimizing confounding effects from land-use intensity.

Soil sampling

A total of 12 composite soil samples (three per farm) were collected from the four selected farms. A stratified random sampling design was applied: within each farm, three cultivation areas of approximately 100 m² were selected at random, and within each area a 10 × 10 m sector representing approximately 75% of the cultivated surface was delineated. Each composite sample (~ 1 kg) was formed by combining five subsamples collected in a zigzag pattern at 1 m intervals and subsequently homogenized using the quartering method (Jang, 2010; Wei et al., 2023). Sampling was performed at a depth of 35–40 cm, corresponding to the rhizosphere (Barra Caracciolo & Terenzi, 2021; Kurek & Majewska, 2014). Samples were collected using stainless-steel tools cleaned with deionized water and ethanol between sites, transferred to labeled polyethylene bags, and transported under refrigeration (~ 4°C).

In the laboratory, samples were oven-dried at 60°C for 48 h to remove moisture while minimizing potential alteration of soil chemical properties (Wei et al., 2023). Dried samples were disaggregated in an agate mortar and sieved through a 63 µm nylon mesh to recover the silt-and-clay fraction, which concentrates metal(loid)s associated with clays, Fe/Mn oxides, and organic matter (Jang, 2010; Sandström et al., 2022; Xia et al., 2022). The < 63 µm fraction was stored in polyethylene containers in the dark until analysis.

Physicochemical characterization

Soil pH, electrical conductivity (EC), and redox potential (Eh) were determined in aqueous suspensions prepared with a 1:2.5 soil-to-water ratio using Type I deionized water (Sandström et al., 2022). Measurements were performed with a HI6221 pH/ORP meter (Hanna Instruments) equipped with a combined pH electrode and an ORP electrode (Ag/AgCl, 3.5 M KCl reference). All Eh values are reported relative to the standard hydrogen electrode (SHE), obtained by adding + 205 mV at 25°C to the values measured against the Ag/AgCl (3.5 M KCl) reference electrode (Nordstrom & Wilde, 2005)

Soil organic matter (SOM) content was determined by loss on ignition (LOI) (Heiri et al., 2001). Approximately 5 g of dried < 63 µm fraction was dried at 105°C for 24 h and then ignited at 500°C for 4 h; SOM (%) was calculated as the mass loss between 105°C and 500°C (Heiri et al., 2001). All measurements were performed in triplicate, and analytical precision was assessed as the relative standard deviation (RSD) between replicates.

Pseudo-total metal(loid) concentrations by portable XRF

Pseudo-total concentrations of As, Cr, Pb, and Zn in the < 63 µm fraction were determined by portable energy-dispersive X-ray fluorescence (pXRF) using a Bruker S1 TITAN spectrometer, following USEPA Method 6200 (USEPA, 2007). The instrument was operated in Soil application mode with the SoilNCDual method, with a total measurement time of 180 s per replicate. Approximately 5 g of dried, sieved soil was packed into a polyethylene sample cup sealed with a 4 µm Prolene film, ensuring sufficient thickness (> 5 mm).

Each sample was measured in three replicates (D01, D02, D03). Mean RSD values were 2.0% for Zn, 6.1% for Cr, 13.2% for As, and 15.0% for Pb, with all four elements detected in 100% of samples. Calibration was verified at the start of each session using the certified Duplex 2205 reference standard; all measurements passed verification. Reported concentrations correspond to the mean of the three replicates.

Sequential extraction by the Tessier method and AAS

Sequential extraction was applied specifically to Pb because this element is environmentally relevant in agricultural soils and its mobility is strongly influenced by pH, sorption sites, carbonates, Fe–Mn oxides, and organic matter. The Tessier procedure was used to operationally partition Pb among fractions with different potential mobility and bioavailability (Tessier et al., 1979; Kumkrong et al., 2022).

Pb fractionation was performed on four selected samples (M-02, M-06, C-02, and C-04), representing both control and mining farms, using the five-step Tessier procedure, starting from 1 g of the dried < 63 µm fraction: (i) exchangeable (EXC), 1 M $MgCl_2$ (pH 7); (ii) bound to carbonates (CAR), 1 M sodium acetate (pH 5); (iii) bound to Fe/Mn oxides (OXI), hydroxylamine hydrochloride in 25% acetic acid at 96°C; (iv) bound to organic matter (ORG), 30% H_2O_2 with ammonium acetate; and (v) residual (RES), acid digestion ($HCl:HNO_3$). Pb in each fraction was quantified by flame atomic absorption spectrometry (Perkin Elmer AAnalyst 300), with a quantification limit of 1.25 mg kg^{-1}.

The analytical consistency of the results was evaluated through an operational mass balance by comparing the sum of Pb recovered in the five Tessier fractions (EXC + CAR + OXI + ORG + RES) with the corresponding total Pb concentration determined by portable X-ray fluorescence (pXRF) in the same < 63 µm soil fraction. Recovery was calculated as: Recovery (%) = [ΣPb fractions / total Pb by pXRF] × 100. This comparison was used as a quality-control criterion to assess the coherence between the sequential extraction procedure and the independently measured total Pb concentration.

The mobility and potential bioavailability of Pb were evaluated using the Risk Assessment Code (RAC), calculated as the percentage of metal retained in the exchangeable and carbonate-bound fractions relative to the sum of all five fractions (Perin et al., 1985; Dung et al., 2013): no risk (< 1%), low (1–10%), medium (11–30%), high (31–50%), and very high (> 50%).

Geochemical speciation modeling

A screening-level thermodynamic interpretation of the potential predominance fields of Pb, Cr, As, and Zn was conducted using PHREEQC (Parkhurst & Appelo, 1999) with the MINTEQ (v4) thermodynamic database. Measured pH and redox potential (Eh, relative to SHE; converted to pe) were used to locate the samples within theoretical stability fields. Because pseudo-total soil concentrations do not represent dissolved concentrations or activities, the diagrams were interpreted as qualitative indicators of potential speciation rather than as direct estimates of mobility, bioavailability, or aqueous equilibrium distributions.

Statistical analysis

All statistical analyses were performed in R version 4.5.2 (R Core Team, 2025), with a significance level of α = 0.05. Given the small sample size (n = 12), non-parametric methods were used throughout. Because the 12 composite samples were nested within four farms, inferential results were interpreted as exploratory rather than as definitive evidence of farm-type effects. Differences between farms with and without mining history were evaluated using the Mann–Whitney U test, and monotonic associations among soil properties and metal(loid) concentrations were assessed using Spearman's rank correlation coefficient (ρ). Measured concentrations were compared with the maximum permissible limits for agricultural soils (MAE-TULSMA, 2015).

3. Results and discussion

Soil physicochemical properties

The soil physicochemical parameters varied within a relatively narrow range across the evaluated farms, defining a common edaphic framework for metal(loid) behavior (Fig. 3; Table 1). Soil pH ranged from 5.15 to 6.06, indicating acidic to slightly acidic conditions. Electrical conductivity (EC) ranged from 13.92 to 40.50 µS/cm, reflecting low-salinity conditions in all samples. Redox potential (Eh) values ranged from 0.06 to 0.10 V, indicating low-redox to slightly oxidizing conditions. Soil organic matter (SOM), estimated

by loss on ignition, ranged from 0.25% to 1.46%, reflecting low organic matter contents across the evaluated soils.

These physicochemical conditions are relevant because pH, Eh, and SOM strongly influence metal(loid) retention, mobility, and potential bioavailability in soils (Bourg & Loch, 1995; Kumpiene et al., 2008; Karimian et al., 2018). Under acidic conditions, the adsorption of divalent metals such as Pb and Zn onto mineral surfaces may decrease, increasing their relative mobility in the soil solution (Hettiarachchi & Pierzynski, 2004; Fernández-Calviño et al., 2010; Tepanosyan et al., 2022). However, the extent of this mobility also depends on the availability of reactive retention phases, including Fe/Mn oxides, clay minerals, carbonates, and organic matter.

The low SOM contents observed in all samples suggest a limited capacity for organic complexation and chelation of metals. Samples with relatively higher SOM may favor greater retention of Pb and Zn through organic functional groups; however, the overall low SOM content indicates that organic matter is unlikely to be the dominant retention mechanism in these soils (Kumpiene et al., 2008). Likewise, the low EC values suggest that salinity does not exert a major control on metal mobility in the evaluated farms. Overall, the physicochemical results indicate that metal(loid) behavior is mainly controlled by acidic pH, low-redox to slightly oxidizing conditions, and limited organic matter content, while salinity appears to play a secondary role.

3.2 Pseudo-total concentrations of heavy metal(loid)s

The pseudo-total concentrations of heavy metal(loid)s showed limited variability across the evaluated soils, with relatively narrow ranges for all analyzed elements (Fig. 4; Table 1). Chromium and Zn were the most abundant elements, with concentrations ranging from 136 to 163 mg/kg and from 118 to 145.33 mg/kg, respectively. In contrast, Pb and As occurred at lower concentrations, ranging from 9.33 to 19 mg/kg for Pb and from 8.00 to 13.33 mg/kg for As. This pattern was observed in both control and mining-history farms, suggesting that metal(loid) distribution is relatively homogeneous across the evaluated agricultural soils.

The limited spatial variability observed in the pseudo-total concentrations suggests that the evaluated soils may share common geochemical controls. This interpretation is consistent with the comparable physicochemical conditions described above and with the geological setting of the study area, where agricultural soils are developed on alluvial materials derived from surrounding lithological units. Comparable monitoring studies show that interpretation of soil metal patterns requires consideration of geological structure, land use, and local geochemical baselines (Krami et al., 2013; Łabaz et al., 2019). In Amazonian environments, metal(loid) distribution can reflect the combined influence of natural geological background, intense weathering, sediment transport, and mining-related inputs, which may complicate the distinction between geogenic and anthropogenic sources when spatial variability is low (Moulatlet et al., 2023; Montoya et al., 2025; Tapia Cordero, 2024). Similar patterns have been reported in mining-influenced tropical systems, where total metal concentrations alone are insufficient to define

source, mobility, or environmental risk without considering soil properties and geochemical partitioning (Ramos et al., 2022).

The Mann–Whitney U test was used to compare soil physicochemical properties and pseudo-total metal(loid) concentrations between control and mining-history farms (Table 2). The results showed a significant difference in pH between both groups, with mining-history soils presenting lower median pH values than control soils ($U = 2.0$, $p = 0.009$). In contrast, no statistically significant differences were observed for EC, Eh, SOM, or the pseudo-total concentrations of Cr, As, Zn, and Pb ($p > 0.05$). These results indicate that, although mining-history farms showed slightly more acidic conditions, metal(loid) concentrations were not statistically differentiated between farm categories. Therefore, the distribution of Cr, As, Zn, and Pb appears to be more strongly associated with shared edaphic and geological conditions than with mining history alone.

Table 1
Soil physicochemical parameters and pseudo-total heavy metal(loid) concentrations in samples from control and mining-history farms.

Farms	Samples	pH	EC (µS/cm)	Eh (V)	SOM (%)	Cr (mg/kg)	As (mg/kg)	Zn (mg/kg)	Pb (mg/kg)
Control	C-01	5.98	24.4	0.06	0.51	163	9.33	127	16
	C-02	6.06	22.5	0.06	0.85	159.33	13.33	140.33	9.33
	C-03	5.61	40.5	0.08	0.74	138.67	10.00	128	12.33
	C-04	5.41	34.3	0.09	0.75	147.33	12.33	118.67	12
	C-05	5.52	13.92	0.09	0.76	151	10.33	120	14.67
	C-06	5.43	22.9	0.09	0.98	149.33	8.67	129	19
Mining	M-01	5.32	35.9	0.10	0.25	159	10.33	125.67	13
	M-02	5.25	19.86	0.09	0.43	147	9.33	133	16
	M-03	5.15	18.77	0.10	0.27	148	8.00	118	15.33
	M-04	5.49	14.32	0.08	1.24	146.67	8.00	119	12.67
	M-05	5.39	19.72	0.09	0.99	155	11.67	145.33	14
	M-06	5.23	29.3	0.09	1.46	136	9.33	125.33	12.67

Table 2
Mann–Whitney U test comparing soil physicochemical properties and pseudo-total metal(loid) concentrations between control and mining-history farms.

Variable	Control median	Mining-history median	U statistic	p-value
pH	5.57	5.29	2.0	0.009
EC (µS/cm)	23.65	19.79	13.0	0.485
Eh (V)	0.085	0.090	8.0	0.102
SOM (%)	0.76	0.71	18.0	1.000
Cr (mg/kg)	150.17	147.50	12.0	0.394
As (mg/kg)	10.17	9.33	10.5	0.257
Zn (mg/kg)	127.50	125.50	16.0	0.818
Pb (mg/kg)	13.50	13.50	15.5	0.748

Spearman correlation analysis was used to explore monotonic relationships among soil physicochemical properties and pseudo-total metal(loid) concentrations (Fig. 5). The strongest and only statistically significant correlation was observed between pH and Eh ($\rho = -0.79$, $p \approx 0.002$), indicating that more acidic soils tended to show higher redox potential values. This relationship suggests that soil acidity and redox conditions are coupled in the evaluated soils, which is environmentally relevant because pH and Eh jointly regulate sorption, precipitation–dissolution reactions, redox transformations, and metal(loid) speciation (Bourg & Loch, 1995; Kumpiene et al., 2008; Karimian et al., 2018). In contrast, no statistically significant correlations were observed between soil properties and pseudo-total metal(loid) concentrations at $\alpha = 0.05$. The strongest non-significant associations involving metal(loid)s were observed between pH and Cr, Eh and Zn, pH and As, and EC and Pb. These results suggest that pseudo-total metal(loid) concentrations are not controlled by a single physicochemical variable, but that metal mobility may still be influenced by the combined effect of soil acidity, redox conditions, organic matter content, and lithological background.

Comparison with the maximum permissible limits (MPLs) established by TULSMA was used as a contextual screening tool rather than as a complete risk assessment. Within this framework, Cr and Zn presented the highest concentrations among the analyzed elements, whereas Pb and As remained at lower levels. However, environmental risk cannot be inferred from pseudo-total concentrations alone because the mobility, bioavailability, and toxicity of metal(loid)s depend on their chemical form, solubility, redox state, and association with reactive soil fractions (Tessier et al., 1979; Vila, 2018; Ramos et al., 2022). Therefore, the interpretation of these concentrations must be complemented with bioavailability and speciation indicators, particularly where soils act as interfaces between natural and human-influenced systems (Monaci & Baroni, 2025).

Pb is particularly relevant from an environmental perspective, not only because of its toxicity and potential transfer through the soil–plant system, but also because its mobility can increase under acidic soil conditions when adsorption onto mineral surfaces, carbonates, Fe/Mn oxides, or organic matter is limited (Hettiarachchi & Pierzynski, 2004; Tepanosyan et al., 2022). Similarly, Zn may become more mobile under acidic conditions due to reduced adsorption onto mineral phases and competition with protons at sorption sites (Fernández-Calviño et al., 2010). In contrast, Cr and As require interpretation in terms of redox-sensitive speciation and interactions with Fe/Al oxide phases, because Cr(III)/Cr(VI) and As(III)/As(V) transformations strongly condition their mobility and toxicity in soils (Pigna et al., 2015; Shahid et al., 2017; Deng et al., 2020; T. Xu et al., 2020). For this reason, the pseudo-total concentration data provide an initial assessment of metal(loid) occurrence, while the sequential extraction and pH–Eh interpretation discussed below provide additional insight into potential mobility and bioavailability.

3.3 Assessment of Pb bioavailability and metal speciation

The sequential extraction results (Fig. 6) indicate that Pb is predominantly associated with the exchangeable fraction (EXC) in the four selected soil samples (M-02, M-06, C-02, and C-04). This fraction represents the most labile and potentially bioavailable pool, as Pb retained in exchangeable sites can be more readily released into the soil solution under changes in pH, ionic strength, or redox conditions (Tessier et al., 1979; Tepanosyan et al., 2022). Pb concentrations in the EXC fraction ranged from 9.72 mg/kg in M-06 to 18.82 mg/kg in C-04. In contrast, Pb was not detected in the carbonate-bound (CAR), Fe/Mn oxide-bound (OXI), or organic matter-bound (ORG) fractions. Minor contributions were observed in the residual fraction (RES) in M-02 and M-06, with values of 1.97 and 3.56 mg/kg, respectively, whereas Pb was not detected in the residual fraction of C-02 and C-04. This distribution suggests that Pb is mainly retained in weakly bound forms rather than incorporated into more stable geochemical fractions.

The predominance of Pb in the EXC fraction indicates high potential mobility and bioavailability under the acidic conditions observed in the evaluated soils. Acidic pH can reduce Pb adsorption onto mineral surfaces and limit retention in carbonate-associated phases, increasing the relative importance of exchangeable forms (Hettiarachchi & Pierzynski, 2004; Kicińska et al., 2022; Tepanosyan et al., 2022). In addition, the low SOM content reported for the evaluated soils suggests a limited capacity for Pb complexation with organic functional groups, which may further contribute to the occurrence of Pb in labile fractions (Kumpiene et al., 2008). These conditions are consistent with the pH–Eh framework described above, where soil acidity and redox conditions appear to act as coupled controls on metal mobility.

The operational mass balance showed variable recoveries between the sum of the Tessier fractions and the pseudo-total Pb concentrations determined by pXRF (Table 3). Recoveries ranged from 86.69% in M-02 to 164.09% in C-02. The mining-history samples showed recoveries close to the expected analytical range, particularly M-02 and M-06, whereas the control samples C-02 and C-04 showed higher recoveries. These differences may reflect sample heterogeneity, matrix effects associated with pXRF measurements, differences between analytical techniques, or uncertainty related to low Pb

concentrations. Therefore, the sequential extraction results should be interpreted as operational fractionation data rather than as absolute total Pb recovery.

Despite the variability in recovery, the Risk Assessment Code (RAC) values were consistently high across the four selected samples. RAC values ranged from 73.19% in M-06 to 100% in C-02 and C-04, placing these samples within the “very high risk” screening category according to the RAC classification (Perin et al., 1985). Given the variable analytical recoveries and the limited subset of four samples, these RAC values should be treated as screening indicators rather than as definitive risk estimates. The result reflects the predominance of Pb in the exchangeable fraction and indicates potentially high mobility and bioavailability under the observed acidic soil conditions. Therefore, the RAC results support the interpretation that Pb availability is controlled more by its labile geochemical partitioning than by pseudo-total concentration alone (Vila, 2018).

Table 3
Summary of Pb recovery and Risk Assessment Code (RAC) for selected soil samples analyzed by Tessier sequential extraction.

Sample	Pb by pXRF (mg/kg)	ΣPb Tessier (mg/kg)	Recovery (%)	RAC (%)	RAC category
M-02	16.00	13.87	86.69	85.80	Very high
M-06	12.67	13.28	104.81	73.19	Very high
C-02	9.33	15.31	164.09	100.00	Very high
C-04	12.00	18.82	156.83	100.00	Very high

Note. RAC was calculated as the percentage of Pb in the exchangeable plus carbonate-bound fractions relative to the sum of all Tessier fractions. The carbonate-bound, Fe/Mn oxide-bound, and organic matter-bound fractions were not detected in the selected samples; therefore, RAC values mainly reflect the exchangeable fraction

The pH–Eh predominance diagrams were used as a screening-level thermodynamic framework to interpret the potential aqueous forms of the analyzed elements under the measured soil conditions (Fig. 7). The sample points occupy a narrow pH–pe interval, with acidic pH and moderately oxidizing conditions. This clustering indicates that control and mining-history farms share a similar geochemical domain. The significant negative correlation between pH and Eh described above also suggests that acidity and redox conditions vary together in the evaluated soils.

For Pb (Fig. 7a), all samples fall within the Pb^{2+} predominance field. The diagram shows that Pb^{2+} is favored across a broad pH–pe range, including near-neutral pH. Thus, the high potential mobility inferred for the evaluated soils should not be attributed to acidity alone. Rather, it reflects the combination of Pb^{2+} predominance, acidic soil conditions, low SOM content, and the dominance of Pb in the exchangeable fraction. At higher pH, Pb^{2+} may still be the dominant aqueous species, but its effective mobility can decrease through stronger adsorption onto mineral surfaces, Fe/Mn oxides, organic matter, or

precipitation with carbonate and phosphate phases (Hettiarachchi & Pierzynski, 2004; Tepanosyan et al., 2022).

For Cr (Fig. 7b), most samples plot within the $Cr(OH)^{2+}$ field, close to other hydrolyzed Cr(III) species. This pattern indicates that Cr is favored in trivalent hydrolyzed forms under the measured conditions. These species are generally less mobile and less toxic than Cr(VI), which is favored under more strongly oxidizing conditions (Shahid et al., 2017; T. Xu et al., 2020; Ju et al., 2022). Cr therefore appears to have lower relative mobility than Pb and Zn in the evaluated soils.

For As (Fig. 7c), the sample points fall mainly within the $H_2AsO_4^-$ field. Arsenic is thermodynamically favored as an oxidized arsenate species under the observed conditions. This does not necessarily imply high mobility, because arsenate can be strongly retained by Fe and Al oxides under acidic to moderately acidic conditions. Its mobility may increase when phosphate competes for sorption sites or when Fe oxides undergo reductive dissolution (Pigna et al., 2015; Deng et al., 2020; Zhuang et al., 2023).

For Zn (Fig. 7d), all samples fall within the Zn^{2+} predominance field. Zn is favored as a free divalent cation, which agrees with the relatively high mobility expected for this element in acidic soils. Its effective mobility may still vary with pH, clay content, Fe/Mn oxides, and organic matter, which can provide sorption sites as pH increases (Fernández-Calviño et al., 2010).

The theoretical predominance diagrams show a clear contrast among the analyzed elements. Pb and Zn are favored as free divalent cations, Cr occurs mainly as hydrolyzed Cr(III) species, and As is favored as $H_2AsO_4^-$. Together with the sequential extraction results, these patterns indicate that metal(loid) mobility is largely controlled by local soil chemistry. Pb shows the strongest evidence of high potential bioavailability, Zn also presents potential mobility, Cr appears less mobile, and As behavior is likely governed by arsenate sorption–desorption processes. The similar position of control and mining-history samples in the diagrams supports the idea that intrinsic soil conditions play a major role in regulating metal(loid) availability in the evaluated farms.

4. Conclusions

The evaluated agricultural soils from the upper Anzu watershed showed limited variability in pseudo-total Pb, Cr, As, and Zn concentrations. No statistically significant differences in metal(loid) concentrations were observed between control and mining-history farms, although mining-history soils presented significantly lower pH values. This pattern suggests that metal(loid) distribution in the evaluated soils is not clearly differentiated by mining history alone and is likely influenced by shared edaphic and lithological conditions.

Soil acidity, redox conditions, low SOM content, and low salinity define the main geochemical framework controlling metal(loid) behavior in the study area. The significant negative correlation between pH and Eh indicates that acidity and redox conditions are coupled in these soils, which is relevant for interpreting metal mobility and speciation. The screening-level pH–Eh diagrams suggested that Pb and Zn are

favored as free divalent cations, Cr occurs mainly as hydrolyzed Cr(III) species, and As is favored as $H_2AsO_4^-$ under the measured conditions.

Pb showed the clearest evidence of high potential bioavailability. Sequential extraction indicated a predominance of Pb in the exchangeable fraction, and RAC values placed the four selected samples within the very high risk screening category. These results show that Pb risk in the evaluated soils is more closely related to its labile partitioning than to pseudo-total concentration alone. Zn also showed potential mobility based on its modeled predominance as Zn^{2+}, whereas Cr appears comparatively less mobile and As mobility is likely regulated by arsenate sorption–desorption processes.

The results highlight the importance of integrating pseudo-total concentrations, soil physicochemical properties, sequential extraction, and pH–Eh speciation to assess metal(loid) mobility and potential bioavailability in tropical agricultural soils. Future work should include direct plant uptake studies, leaching tests, mineralogical characterization, and a broader spatial sampling design to better constrain metal(loid) transfer pathways and distinguish geogenic from anthropogenic contributions.

Declarations

Funding Declaration

The authors received no financial support for the research, authorship, and/or publication of this article.

Author Contribution

Y.B. conceived and designed the study, planned and conducted the field sampling campaign, performed all laboratory analyses (physicochemical characterization, portable X-ray fluorescence, and Tessier sequential extraction with atomic absorption spectrophotometry), carried out the data analysis and statistical processing in R, constructed and interpreted the Pourbaix (Eh–pH) diagrams, prepared all figures and tables, and wrote the original draft of the manuscript. S.B.L. supervised the research, provided overall scientific guidance throughout the study, contributed to the conceptualization and methodological design, critically reviewed and edited successive versions of the manuscript, and acted as corresponding author. O.G. made substantial intellectual contributions to the manuscript, including critical review of the geological framework and the geochemical interpretation of the results, and provided substantive revisions to the draft. S.J.O., C.G.C., A.G., and E.T. contributed to the review and editing of the manuscript. All authors read and approved the final version of the manuscript and agree to be accountable for all aspects of the work.

Acknowledgement

We gratefully acknowledge the communities of Carlos Julio Arosemena Tola canton for their collaboration and support throughout the development of this study. We extend our sincere appreciation

to Kevin Salazar and Fundación Maquita for their assistance with territorial reconnaissance and access to the study area. We also thank Agustín Bermello, Joao Calle, and Elizabeth Guadamud for their valuable support during field sampling campaigns and field logistics.

Data Availability

All the data is in the manuscript; if you need additional information, you can write to the corresponding author.

References

1. Angon, P. B., Islam, M. S., KC, S., Das, A., Anjum, N., Poudel, A., & Suchi, S. A. (2024). Sources, effects and present perspectives of heavy metals contamination: Soil, plants and human food chain. *Heliyon*, *10*(7), e28357. https://doi.org/10.1016/j.heliyon.2024.e28357
2. Aspden, J. A., Harrison, S. H., & Rundle, C. C. (1992). New geochronological control for the tectono-magmatic evolution of the metamorphic basement, Cordillera Real and El Oro Province of Ecuador. *Journal of South American Earth Sciences*, *6*(1), 77–96. https://doi.org/10.1016/0895-9811(92)90019-U
3. Baby, P., Rivadeneira, M., & Barragan, R. (2004). *La cuenca oriente: geologia y petroleo*. Convenio IFEA-IRD-Petroecuador.
4. Barra Caracciolo, A., & Terenzi, V. (2021). Rhizosphere microbial communities and heavy metals. *Microorganisms*, *9*(7). https://doi.org/10.3390/microorganisms9071462
5. Bourg, A. C. M., & Loch, J. P. G. (1995). *Mobilization of Heavy Metals as Affected by pH and Redox Conditions BT - Biogeodynamics of Pollutants in Soils and Sediments: Risk Assessment of Delayed and Non-Linear Responses* (W. Salomons & W. M. Stigliani (eds.); pp. 87–102). Springer Berlin Heidelberg. https://doi.org/10.1007/978-3-642-79418-6_4
6. Campillo-Cora, C., Rodríguez-Seijo, A., Pérez-Rodríguez, P., Fernández-Calviño, D., & Santás-Miguel, V. (2025). Effect of heavy metal pollution on soil microorganisms: Influence of soil physicochemical properties. A systematic review. *European Journal of Soil Biology*, *124*. https://doi.org/10.1016/j.ejsobi.2024.103706
7. Capparelli, M. V., Moulatlet, G. M., Abessa, D. M. de S., Lucas-Solis, O., Rosero, B., Galarza, E., Tuba, D., Carpintero, N., Ochoa-Herrera, V., & Cipriani-Avila, I. (2020). An integrative approach to identify the impacts of multiple metal contamination sources on the Eastern Andean foothills of the Ecuadorian Amazonia. Science of the Total Environment, 709, 136088. https://doi.org/10.1016/j.scitotenv.2019.136088
8. Fernández-Calviño, D., Pérez-Novo, C., Bermúdez-Couso, A., López-Periago, E., & Arias-Estévez, M. (2010). Batch and stirred flow reactor experiments on Zn sorption in acid soils: Cu competition. Geoderma, 159(3–4), 417–424. https://doi.org/10.1016/j.geoderma.2010.09.007

9. Christophoul, F., Baby, P., & Dávila, C. (2002). Stratigraphic responses to a major tectonic event in a foreland basin: the Ecuadorian Oriente Basin from Eocene to Oligocene times. *Tectonophysics*, *345*(1), 281–298. https://doi.org/10.1016/S0040-1951(01)00217-7
10. Conali. (2020). *Geoportal de Catastro Minero*.
11. Deng, Y., Weng, L., Li, Y., Chen, Y., & Ma, J. (2020). Redox-dependent effects of phosphate on arsenic speciation in paddy soils. Environmental Pollution, 264, 114783. https://doi.org/10.1016/j.envpol.2020.114783
12. Dung, T. T. T., Cappuyns, V., Swennen, R., & Phung, N. K. (2013). From geochemical background determination to pollution assessment of heavy metals in sediments and soils. *Reviews in Environmental Science and Biotechnology*, *12*(4), 335–353. https://doi.org/10.1007/s11157-013-9315-1
13. Galarza, E., Cabrera, M., Espinosa, R., Espitia, E., Moulatlet, G. M., & Capparelli, M. V. (2021). Assessing the Quality of Amazon Aquatic Ecosystems with Multiple Lines of Evidence: The Case of the Northeast Andean Foothills of Ecuador. *Bulletin of Environmental Contamination and Toxicology*, *107*(1), 52–61. https://doi.org/10.1007/s00128-020-03089-0
14. Gutiérrez, E. G., Horton, B. K., Vallejo, C., Jackson, L. J., & George, S. W. M. (2019). Chapter 9 - Provenance and geochronological insights into Late Cretaceous-Cenozoic foreland basin development in the Subandean Zone and Oriente Basin of Ecuador. In B. K. Horton & A. Folguera (Eds.), *Andean Tectonics* (pp. 237–268). Elsevier. https://doi.org/10.1016/B978-0-12-816009-1.00011-3
15. Guzman, O., & Campos, C. (2024). *Geociencias en la Amazonía Ecuatoriana: Aportes a la Planificación Sostenible*. CEDIA-Universidad Regional Amazónica Ikiam. https://doi.org/10.48661/w6dc-q685
16. Heiri, O., Lotter, A. F., & Lemcke, G. (2001). Loss on ignition as a method for estimating organic and carbonate content in sediments: reproducibility and comparability of results. *Journal of Paleolimnology*, *25*(1), 101–110. https://doi.org/10.1023/A:1008119611481
17. Hettiarachchi, G. M., & Pierzynski, G. M. (2004). Soil lead bioavailability and in situ remediation of lead-contaminated soils: A review. Environmental Progress, 23(1), 78–93. https://doi.org/10.1002/ep.10004
18. Huatatoca-mamallacta, S., Simbaña-tasiguano, M., Granja-guato, D., Espín, R., Lima, L. De, Cisneros, P., Salgado-revelo, A., Almeida, E., & Tana, A. (2025). *Unveiling the Igneous Geodiversity of the Shunku Rumi Geosite for Geoeducation and Geotourism Actions in the Napo Sumaco UNESCO Global Geopark (Ecuador)*. 1–23.
19. INAMHI. (2025). *Boletín de predicción climática*. 1–7. https://servicios.inamhi.gob.ec/clima/
20. Jang, M. (2010). Application of portable X-ray fluorescence (pXRF) for heavy metal analysis of soils in crop fields near abandoned mine sites. *Environmental Geochemistry and Health*, *32*(3), 207–216. https://doi.org/10.1007/s10653-009-9276-z
21. Jiménez, S., Segovia, K., Martínez, M., Ortega, M., Bolonio, D., García, I., & Salgado, B. (2021). *Human Health Risk Assessment for Exposure to Potentially Toxic Elements in Polluted Rivers in the Ecuadorian*

Amazon.

22. Ju, L., Jiao, Z., Ge, S., Zhan, W., Liu, Y., Ren, Q., Liao, Q., Yang, Z., & Wang, Y. (2022). Formation, stability and mobility of soluble Cr(III) during Cr(VI) reduction by Pannonibacter phragmitetus BB. Environmental Technology & Innovation, 27, 102496. https://doi.org/10.1016/j.eti.2022.102496
23. Karimian, N., Johnston, S. G., & Burton, E. D. (2018). Antimony and arsenic partitioning during Fe2+-induced transformation of jarosite under acidic conditions. *Chemosphere*, *195*, 515–523. https://doi.org/10.1016/j.chemosphere.2017.12.106
24. Kicińska, A., Pomykała, R., & Izquierdo-Diaz, M. (2022). Changes in soil pH and mobility of heavy metals in contaminated soils. European Journal of Soil Science, 73(2), e13203. https://doi.org/10.1111/ejss.13203
25. Krami, L. K., Amiri, F., Sefiyanian, A., Shariff, A. R. B. M., Tabatabaie, T., & Pradhan, B. (2013). Spatial patterns of heavy metals in soil under different geological structures and land uses for assessing metal enrichments. Environmental Monitoring and Assessment, 185(12), 9871–9888. https://doi.org/10.1007/s10661-013-3298-9
26. Kumkrong, P., Dy, E., Tyo, D. D., Jiang, C., Gedara Pihilligawa, I., Kingston, D., & Mercier, P. H. J. (2022). Investigation of metal mobility in gold and silver mine tailings by single-step and sequential extractions. Environmental Monitoring and Assessment, 194(6), 423. https://doi.org/10.1007/s10661-022-10054-3
27. Kumpiene, J., Lagerkvist, A., & Maurice, C. (2008). Stabilization of As, Cr, Cu, Pb and Zn in soil using amendments: A review. Waste Management, 28(1), 215–225. https://doi.org/10.1016/j.wasman.2006.12.012
28. Kurek, E., & Majewska, M. (2014). Microbially Mediated Transformations of Heavy Metals in Rhizosphere. *Toxicity of Heavy Metals to Legumes and Bioremediation*, 1–244. https://doi.org/10.1007/978-3-7091-0730-0
29. Łabaz, B., Kabała, C., & Waroszewski, J. (2019). Ambient geochemical baselines for trace elements in Chernozems—approximation of geochemical soil transformation in an agricultural area. Environmental Monitoring and Assessment, 191(1), 19. https://doi.org/10.1007/s10661-018-7133-1
30. Litherland, M., & Viteri, G. (1994). *Los cinturones metamórficos del Ecuador*.
31. MAE-TULSMA. (2015). *Texto Unificado de Legislación Secundaria Medio Ambiental. Ministerio de Ambiente de Ecuador*.
32. Monaci, F., & Baroni, D. (2025). Spatial distribution and ecological risk of potentially toxic elements in peri-urban soils of a historically industrialised area. Environmental Monitoring and Assessment, 197(8), 948. https://doi.org/10.1007/s10661-025-14389-5
33. Montoya, J. V., Ríos-Touma, B., Lujan, N. K., Sánchez, F., Proaño, A., Tejera, E., Jimenes-Vargas, K., Sánchez, L., & Cuesta, F. (2025). Spatiotemporal distributions and potential sources of sediment and waterborne heavy metals in lowland lakes and rivers of the Ecuadorian Amazon. Environmental Monitoring and Assessment, 197(9), 1022. https://doi.org/10.1007/s10661-025-14451-2

34. Moulatlet, G. M., Yacelga, N., Rico, A., Mora, A., Hauser-Davis, R. A., Cabrera, M., & Capparelli, M. V. (2023). A systematic review on metal contamination due to mining activities in the Amazon basin and associated environmental hazards. *Chemosphere*, *339*(August), 139700. https://doi.org/10.1016/j.chemosphere.2023.139700
35. Nordstrom, D. K., & Wilde, F. D. (2005). Reduction-Oxidation Potential (Electrode Method). In *National Field Manual for the Collection of Water-Quality Data* (Version 1.2, Techniques of Water-Resources Investigations, Book 9, Chapter A6.5). U.S. Geological Survey. https://doi.org/10.3133/twri09A6.5
36. Parkhurst, D. L., & Appelo, C. A. J. (1999). User's guide to PHREEQC (Version 2): A computer program for speciation, batch-reaction, one-dimensional transport, and inverse geochemical calculations. In *Water-Resources Investigations Report* (Issues 99–4259). U.S. Geological Survey.
37. Perin, G., Craboledda, L., Lucchese, M., Cirillo, R., Dotta, L., Zanette, M. L., & Orio, A. A. (1985). Heavy metal speciation in the sediments of Northern Adriatic Sea: A new approach for environmental toxicity determination. In Heavy Metals in the Environment (Vol. 2, pp. 454–456).
38. Pigna, M., Caporale, A. G., Cavalca, L., Sommella, A., & Violante, A. (2015). Arsenic in the soil environment: Mobility and phytoavailability. Environmental Engineering Science, 32(7), 551–563. https://doi.org/10.1089/ees.2015.0018
39. R Core Team. (2025). R: A language and environment for statistical computing. R Foundation for Statistical Computing. https://www.R-project.org/
40. Ramos, C., Ruales, J., Rivera-Parra, J. L., Sakakibara, M., & Díaz, X. (2022). Sustainability of Cocoa (Theobroma cacao) Cultivation in the Mining District of Ponce Enríquez: A Trace Metal Approach. *International Journal of Environmental Research and Public Health*, *19*(21). https://doi.org/10.3390/ijerph192114369
41. Ríos Guayasamín, P. D., Smith, S. M., & Thomas, S. C. (2024). Biochar effects on NTFP-enriched secondary forest growth and soil properties in Amazonian Ecuador. *Journal of Environmental Management*, *350*(January 2023). https://doi.org/10.1016/j.jenvman.2023.119068
42. Rivera-Rhon, R. A., & Bravo-Grijalva, C. E. (2023). Gobernanzas criminales y enclaves productivos de la minería ilegal en Ecuador. *Revista Logos Ciencia & Tecnología*, *15*(2), 49–69. https://doi.org/10.22335/rlct.v15i2.1734
43. Sandström, H., Reeder, S., Bartha, A., Birke, M., Berge, F., Davidsen, B., Grimstvedt, A., Hagel-Brunnström, M-L., Kantor, W., Kallio, E., Klaver, G., Lucivjansky, P., Mackovych, D., Mjartanova, H., van Os, B., Paslawski, P., & Popiolek, E. (2022). *Sample preparation and analysis*. 51–60. https://doi.org/10.1007/978-3-030-56733-0_4
44. Shahid, M., Shamshad, S., Rafiq, M., Khalid, S., Bibi, I., Niazi, N. K., Dumat, C., & Rashid, M. I. (2017). Chromium speciation, bioavailability, uptake, toxicity and detoxification in soil-plant system: A review. Chemosphere, 178, 513–533. https://doi.org/10.1016/j.chemosphere.2017.03.074
45. Strand, J., Soares-Filho, B., Costa, M. H., Oliveira, U., Ribeiro, S. C., Pires, G. F., Oliveira, A., Rajão, R., May, P., van der Hoff, R., Siikamäki, J., da Motta, R. S., & Toman, M. (2018). Spatially explicit valuation

of the Brazilian Amazon Forest's Ecosystem Services. *Nature Sustainability*, *1*(11), 657–664. https://doi.org/10.1038/s41893-018-0175-0

46. Tapia Cordero, E. E. (2024). *Estimación de niveles de fondo geoquímico de elementos tóxicos en sedimentos fluviales en la cuenca alta del río Napo-Ecuador*. *October*.
47. Tepanosyan, G., Pipoyan, D., Beglaryan, M., & Sahakyan, L. (2022). Compositional features of Pb in agricultural soils and geochemical associations conditioning Pb contents in plants. Chemosphere, 306, 135492. https://doi.org/10.1016/j.chemosphere.2022.135492
48. Tessier, A., Campbell, P. G. C., & Bisson, M. (1979). Sequential Extraction Procedure for the Speciation of Particulate Trace Metals. *Analytical Chemistry*, *51*(7), 844–851. https://doi.org/10.1021/ac50043a017
49. USEPA. (2007). SW-846 Test Method 6200: Field Portable X-Ray Fluorescence Spectrometry for the Determination of Elemental Concentrations in Soil and Sediment. In *Test Methods for Evaluating Solid Waste, Physical/Chemical Methods (SW-846)*. United States Environmental Protection Agency. https://www.epa.gov/hw-sw846/sw-846-test-method-6200-field-portable-x-ray-fluorescence-spectrometry-determination
50. Vasco-Viteri, S., Cabrera, M., Pérez-González, A., Hauser-Davis, R. A., Moulatlet, G. M., & Capparelli, M. V. (2023). Metal bioaccumulation and genotoxicity in Oreochromis niloticus reared in farming pools influenced by mining activities in Napo, in the Ecuadorian Amazonia. *Chemosphere*, *335*, 139157. https://doi.org/10.1016/j.chemosphere.2023.139157
51. Vera-Jaramillo, C., Campos, C., Vera, D., Coral, C., Correa-Jaramillo, C., Jaramillo, S. J. N., Zuñiga, R. G., & Guzman, O. (2026). Petrographic and Mineralogical Characterization of the Abitagua Batholith at the "Waysa Yacu and Jatun Yacu River" Geosite of the Napo Sumaco UNESCO Global Geopark in the Ecuadorian Amazon. *Geoheritage*, *18*(2), 96. https://doi.org/10.1007/s12371-026-01321-7
52. Vera, D., Tasiguano, M. S., Guzmán, O., & Cabascango, E. (2023). Quantitative Assessment of Geodiversity in Ecuadorian Amazon — Case Study: Napo Sumaco Aspiring UNESCO Geopark. *Geoheritage*. https://doi.org/10.1007/s12371-023-00792-2
53. Vila, M. L. (2018). *Bioavailability of heavy metals in contaminated soils*. *3*, 1–13.
54. Vilar, S., Gutiérrez, A., Antezana, J., Carral, P., & Álvarez, A. (2003). Estudio comparativo diferentes métodos de extracción secuencial para metales pesados en suelos. *Boletin Geologico y Minero*, *114*(4), 453–461.
55. von Gunten, K. (2024). Chapter 4 - Assessment of heavy metal stability in biochar-treated soil. In Z. Shen (Ed.), *Biochar Application in Soil to Immobilize Heavy Metals* (pp. 81–129). Elsevier. https://doi.org/10.1016/B978-0-323-85459-7.00005-7
56. Wang, X., Cairang, S., Du, J., Wei, Z. Bin, Wu, Q. T., Hu, L., & Xu, M. (2025). A Large-Scale Assessment of Soil Heavy Metal Pollution Using Field-Collected Earthworms as Bio-Indicators in Shaoguan, South China [Research-article]. *Environment and Health*, *3*(6), 616–625. https://doi.org/10.1021/envhealth.4c00249

57. Wei, C., Zhang, Y., Zuo, X., Wan, C., & Wang, Z. (2023). Assessment of Zn, Pb and Cd in Soil around an MSW Incineration Plant: Using Risk Assessment and Multivariate Statistical Techniques. *Processes*, *11*(11). https://doi.org/10.3390/pr11113175
58. Woszczyk, M., Spychalski, W., & Boluspaeva, L. (2018). Trace metal (Cd, Cu, Pb, Zn) fractionation in urban-industrial soils of Ust-Kamenogorsk (Oskemen), Kazakhstan—implications for the assessment of environmental quality. Environmental Monitoring and Assessment, 190(6), 362. https://doi.org/10.1007/s10661-018-6733-0
59. Xu, T., Nan, F., Jiang, X., Tang, Y., Zeng, Y., Zhang, W., & Shi, B. (2020). Effect of soil pH on the transport, fractionation, and oxidation of chromium(III). Ecotoxicology and Environmental Safety, 195, 110459. https://doi.org/10.1016/j.ecoenv.2020.110459
60. Xia, F., Fan, T., Chen, Y., Ding, D., Wei, J., Jiang, D., & Deng, S. (2022). Prediction of Heavy Metal Concentrations in Contaminated Sites from Portable X-ray Fluorescence Spectrometer Data Using Machine Learning. *Processes*, *10*(3). https://doi.org/10.3390/pr10030536
61. Zhuang, F., Huang, J., Li, H., Peng, X., Xia, L., Zhou, L., Zhang, T., Liu, Z., He, Q., Luo, F., Yin, H., & Meng, D. (2023). Biogeochemical behavior and pollution control of arsenic in mining areas: A review. Frontiers in Microbiology, 14, 1043024. https://doi.org/10.3389/fmicb.2023.1043024

Figures

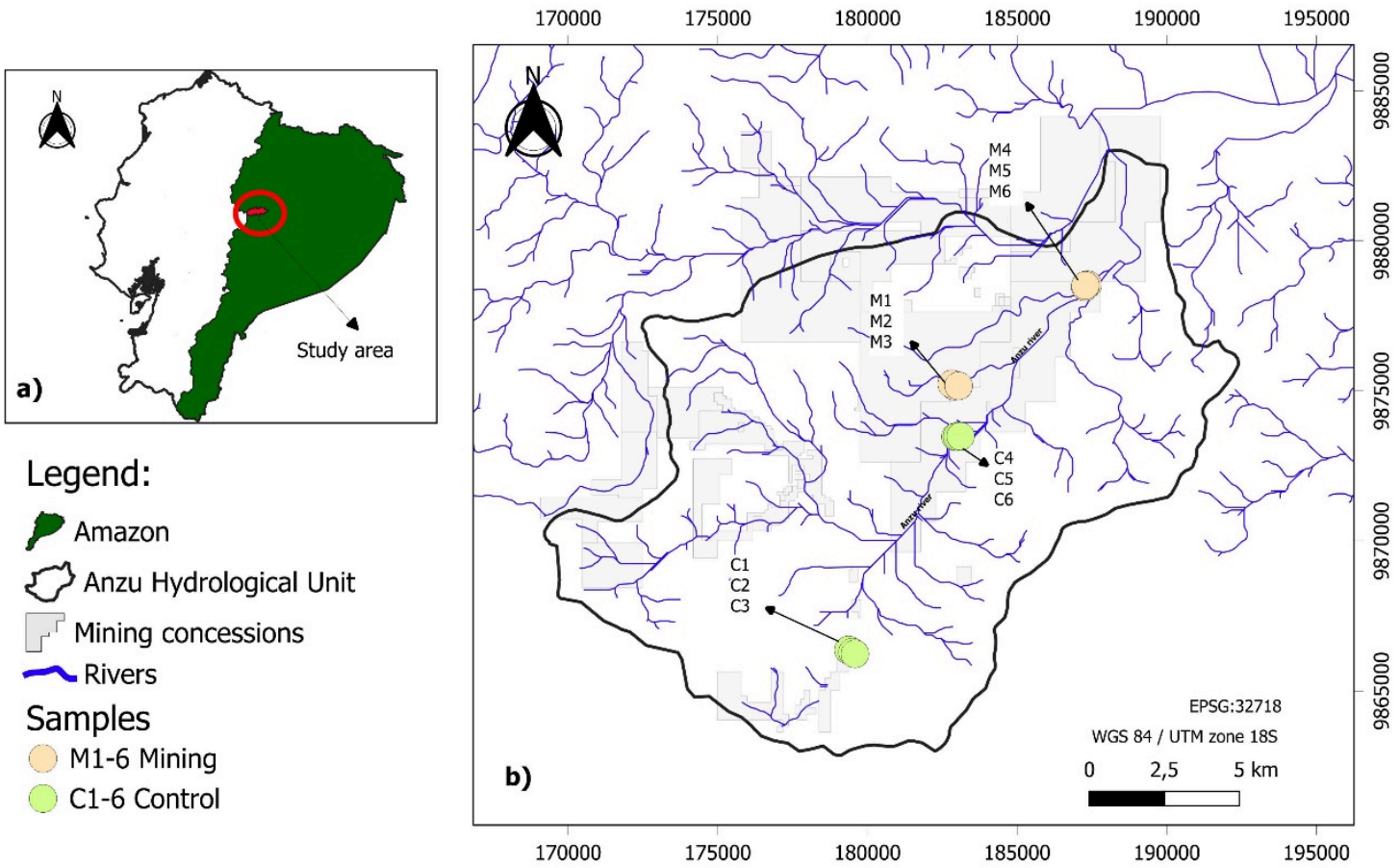


Figure 1

(a) Study area in the Ecuadorian Amazon, and (b) sampling locations

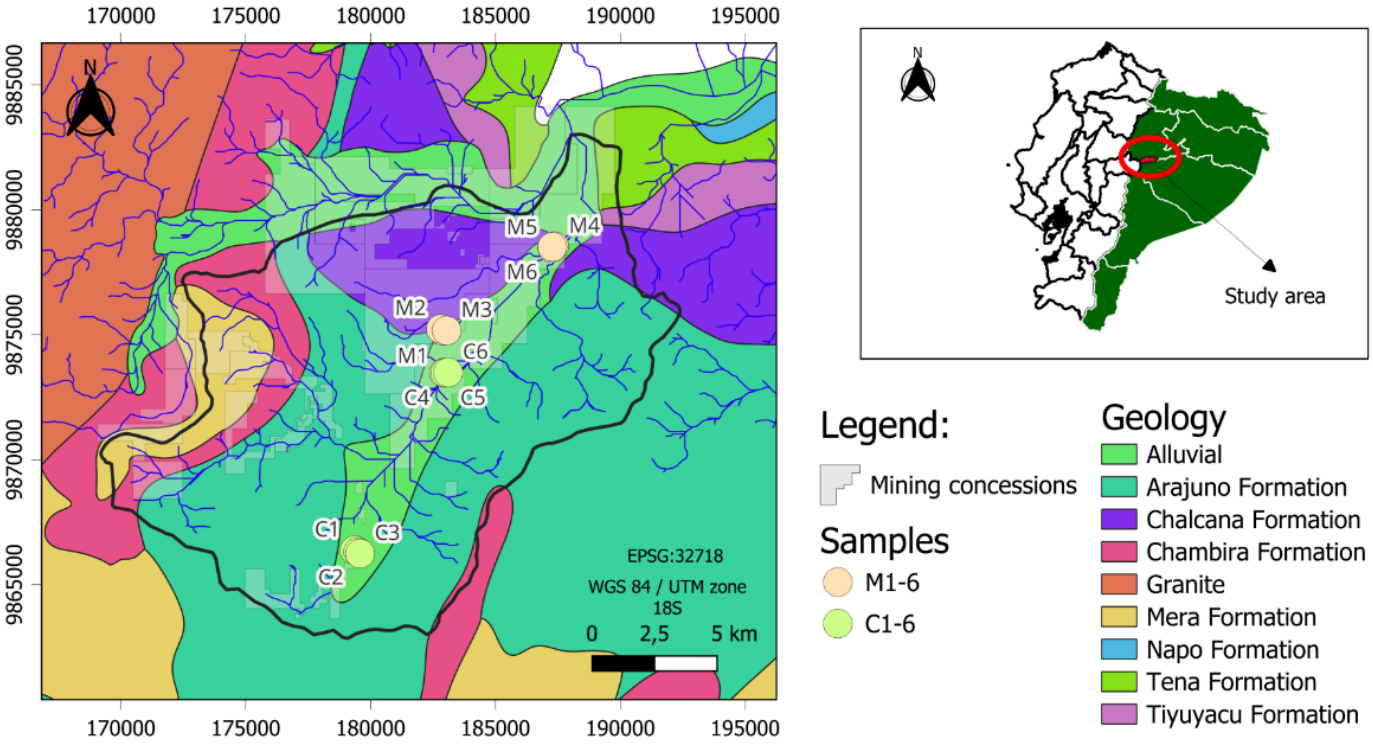


Figure 2

Geological map showing the location of the study farms, mining concession areas, and the hydrographic network in the Ecuadorian Amazon

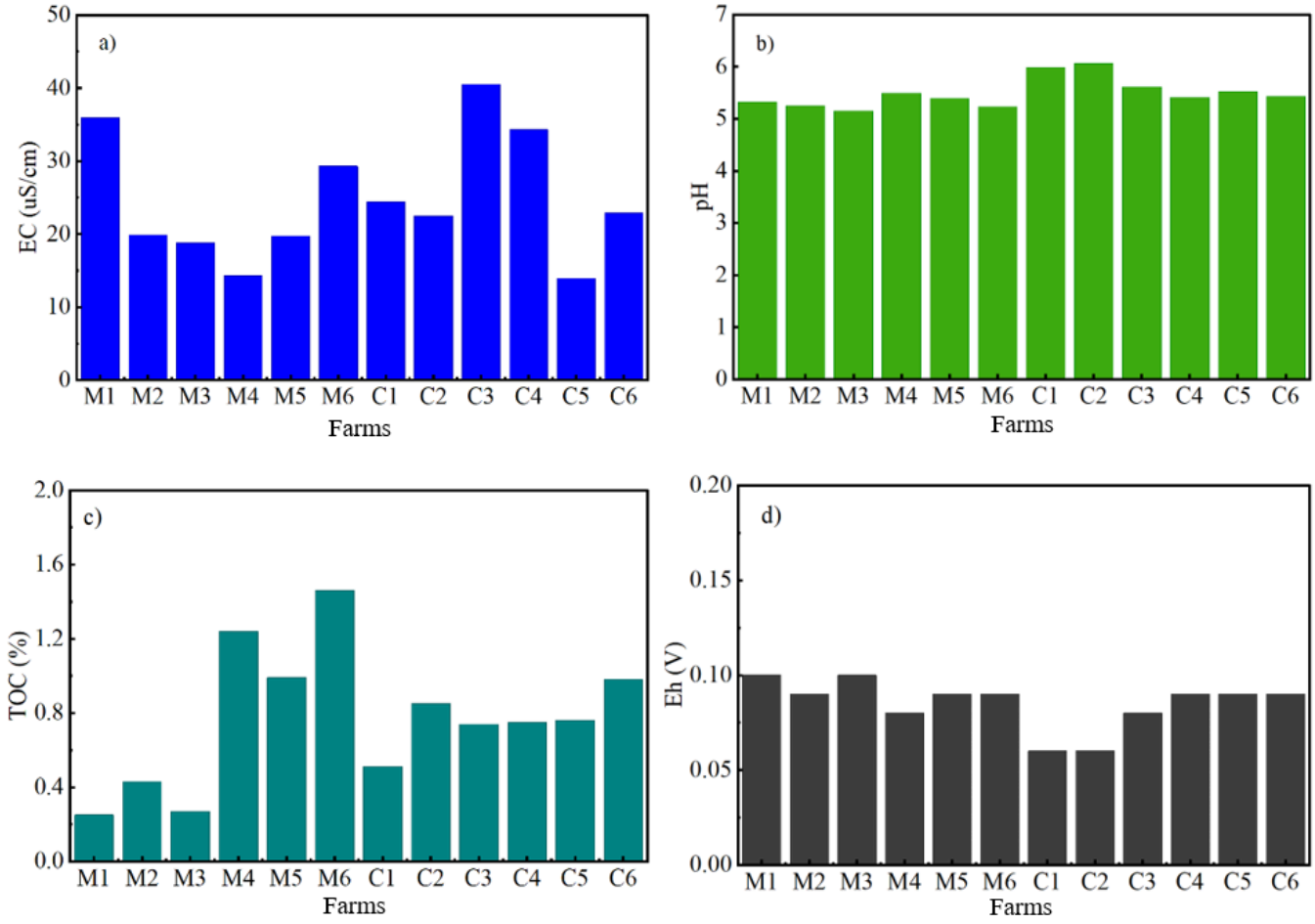


Figure 3

Distribution of soil physicochemical parameters: (a) EC, (b) pH, (c) Eh, and (d) SOM in samples from the evaluated farms

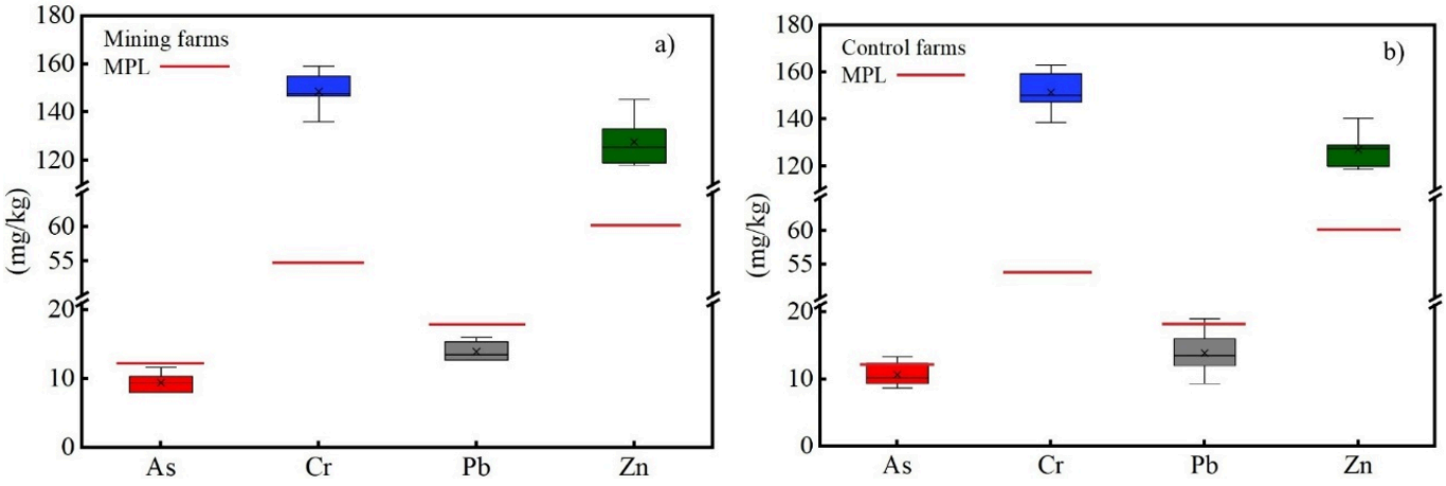


Figure 4

Boxplots of pseudo-total heavy metal(loid) concentrations (As, Cr, Pb, and Zn) in soils from (a) mining-history and (b) control farms, compared with the maximum permissible levels (MPLs) established by TULSMA

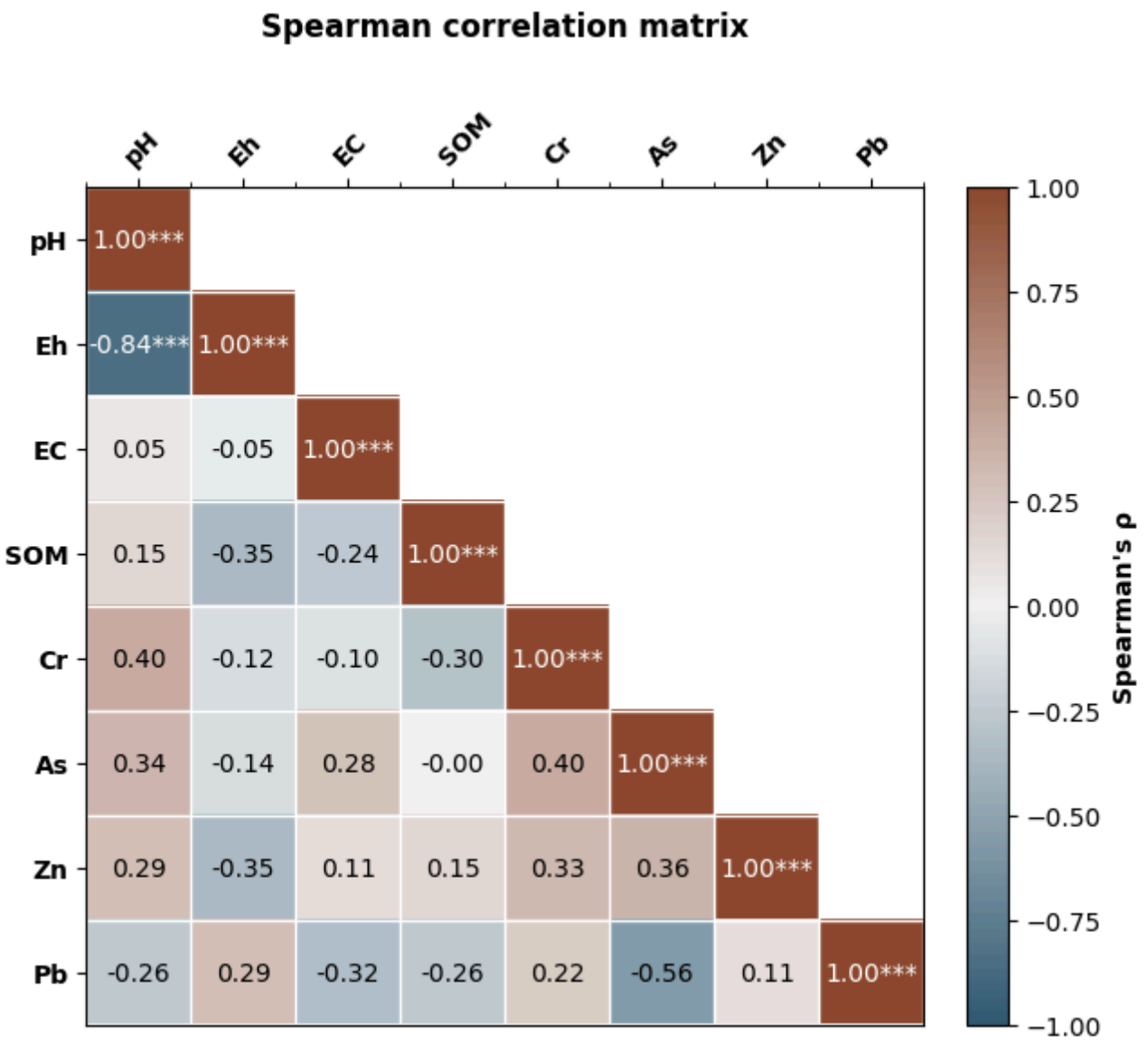


Figure 5

Spearman correlation matrix among soil physicochemical properties and pseudo-total metal(loid) concentrations. The matrix includes pH, EC, Eh, SOM, Cr, As, Zn, and Pb. Color intensity indicates the strength and direction of the Spearman correlation coefficient (ρ). Non-significant correlations should be interpreted as exploratory patterns due to the limited sample size

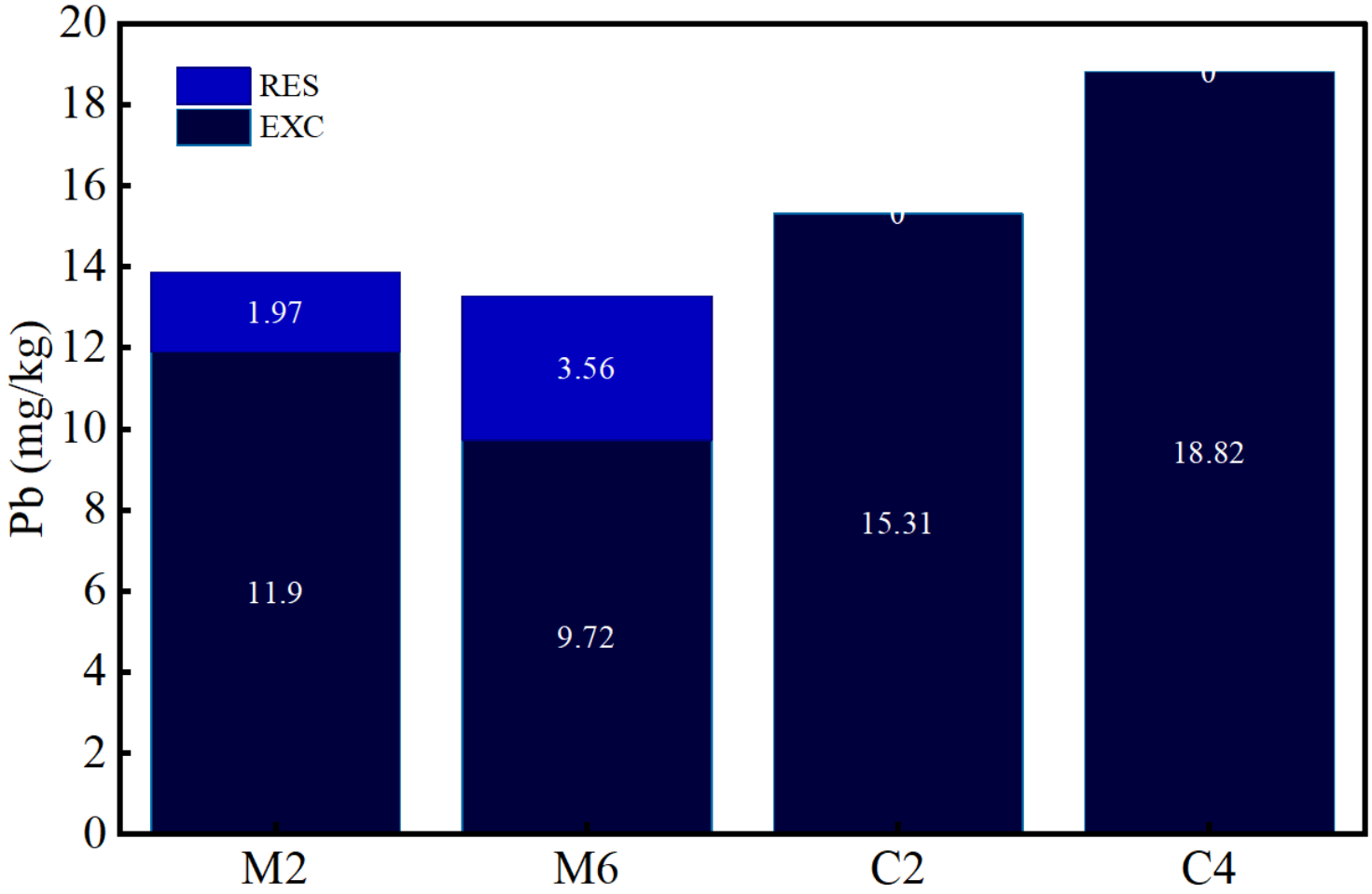


Figure 6

Tessier sequential extraction of Pb in selected soil samples. Fractions: EXC = exchangeable, CAR = carbonate-bound, OXI = Fe/Mn oxide-bound, ORG = organic matter-bound, and RES = residual

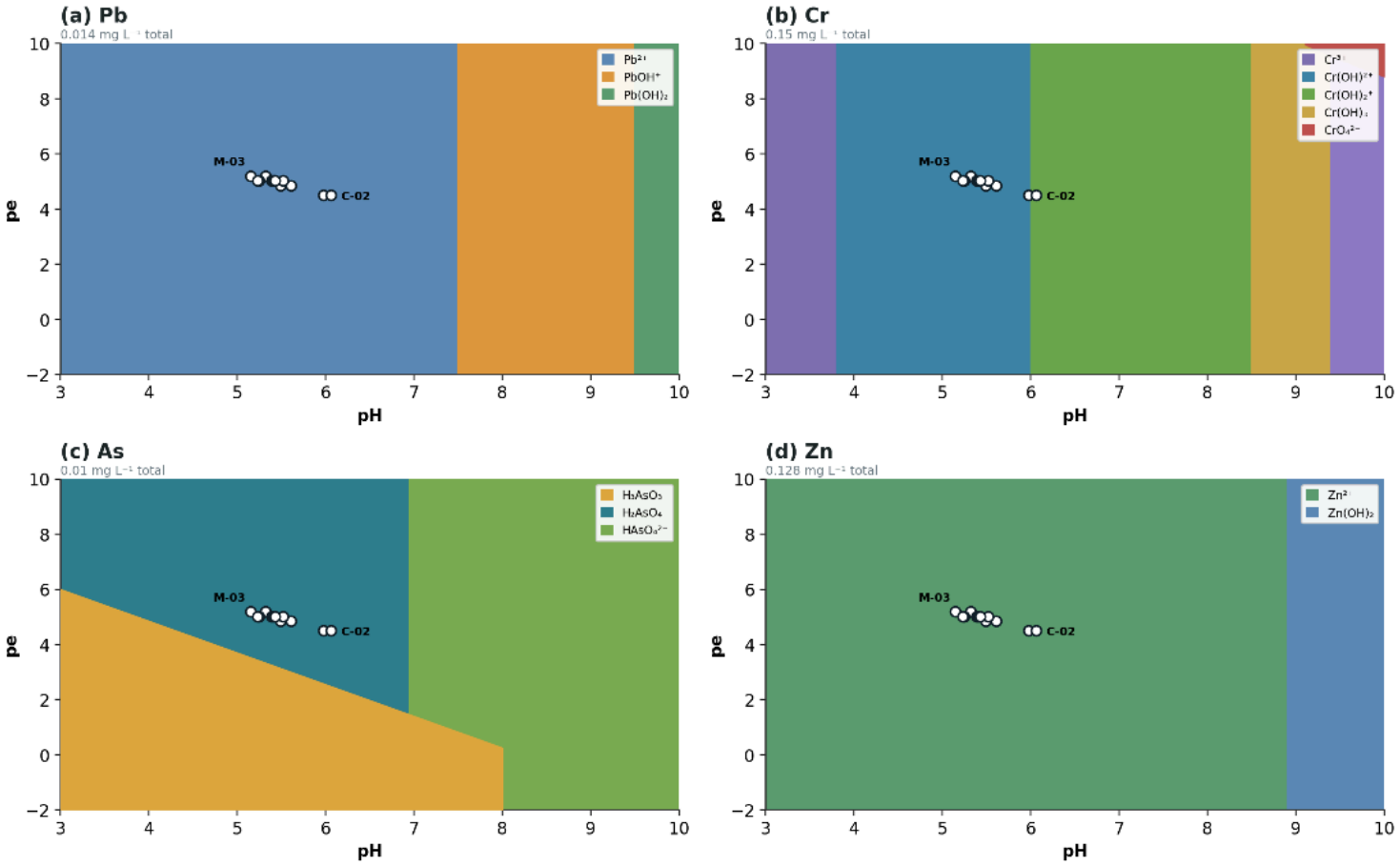


Figure 7

Pourbaix diagrams for (a) Pb, (b) Cr, (c) As, and (d) Zn under the pH–Eh conditions measured in the evaluated soils